A Dynamic Matrix Controller with Feedforward for Flow Field in Intermittent Transonic Wind Tunnels

DU Ning, ZHU Wenjie, YAO Dan, ZOU Xinlei, QIN Jianhua*

High Speed Aerodynamic Institute, China Aerodynamics Research and Development Center, Mianyang 621000, P. R. China

(Received 5 June 2025; revised 29 November 2025; accepted 31 January 2026)

Abstract: Intermittent transonic wind tunnels demand high-precision and stable control of Mach number and stagnation pressure during the variation of model angle of attack, while the traditional proportional integral derivative (PID) control strategy fails to achieve the Mach number control error target of 0.001 and is inept at resisting flow field disturbances caused by rapid changes in angle of attack. Aiming at this problem, this study takes the intermittent transonic wind tunnel of China Aerodynamics Research and Development Center as the research object and optimizes the wind tunnel control system for its characteristics of multi-input multi-output (MIMO), large time delay and nonlinearity. First, the control system structure is reconstructed by introducing ejection pressure as a controlled variable to reduce the time lag from the main pressure regulating valve to the test section, and selecting static pressure instead of Mach number as a controlled variable to weaken the nonlinear coupling between Mach number and static pressure. Second, based on the first-order plus dead time process model of the wind tunnel, a MIMO dynamic matrix controller (DMC) for wind tunnel flow field is designed. Considering the predictable nature of angle-of-attack changes, a feedforward compensation strategy is integrated into the DMC to mitigate the pressure disturbance in the test section caused by the variation of angle of attack. Third, a complete tuning strategy for DMC parameters including sampling time, prediction horizon, control horizon and weight coefficients is formulated according to the wind tunnel model parameters under different Mach numbers. Experimental validations through practical blowing tests are carried out at Mach numbers of 0.578, 0.675, 0.714 and 0.822 to compare the control performance of the proposed feedforward DMC strategy with the traditional PID control and DMC without feedforward compensation. The results show that the proposed strategy stably controls the Mach number error within 0.001, and significantly improves the stagnation pressure control accuracy and anti-disturbance capability of the wind tunnel flow field. Moreover, the strategy exhibits excellent repeatability and robustness under different Mach number conditions. This study effectively solves the problem of high-precision flow field control under the rapid change of angle of attack in intermittent transonic wind tunnels, and provides a technical reference for the flow field control of complex fluid test devices such as hypersonic wind tunnels.

Key words: intermittent transonic wind tunnel; flow field control; dynamic matrix controller(DMC); feedforward compensation; multi-input multi-output(MIMO) system; parameter tuning

CLC number: V211.74 **Document code:** A **Article ID:** 1005-1120(2026)01-0055-18

0 Introduction

Wind tunnels are important simulation platforms for investigating the laws of airflow, the aerodynamic characteristics of aerospace vehicles and other fast moving ground objects[1-4]. Aerodynamic data of scale models are measured at a given Mach number, stagnation pressure, static pressure, temperature, and angle of attack during wind tunnel tests[5-8].

In wind tunnel tests, disturbance is usually caused by test requirements. For example, chang-

*Corresponding author, E-mail address: allwillwell@foxmail.com.

How to cite this article: DU Ning, ZHU Wenjie, YAO Dan, et al. A dynamic matrix controller with feedforward for flow field in intermittent transonic wind tunnels[J]. Transactions of Nanjing University of Aeronautics and Astronautics, 2026, 43(1): 55-72.

http://dx.doi.org/10.16356/j.1005-1120.2026.01.005

ing the angle of attack of scale models will lead to the flow fields deviating from their set state. Hence, the wind tunnel flow field proves to be a highly complex plant. This complexity stems from the coupling between valves[9-10], including a large lag in the valves' effect on the controlled pressure, non-ideal gas behavior, and uncertainties in the flow characteristics of the control valves[11]. Wind tunnel testing demands that controllers are capable of achieving high precision and effectively rejecting disturbances within constrained timeframes. Consequently, advanced control systems with robust performance characteristics are essential for wind tunnel applications.

Some kinds of controllers and control methods have been studied for wind tunnel flow field. By assuming the disturbance of the Mach number is triangular, Soeterboek et al.[3] proposed the unified predictive controller for the Mach number in the high-speed wind tunnel of the National Aerospace Laboratory in Amsterdam. Miwa et al.[12] used the governing equations of the tunnel by assuming choked flow in the control valve of a supersonic blow-down wind tunnel and nominal values for stagnation temperatures and pressures for a fixed throat setting, and designed a linear quadratic Gaussian (LQG)/loop transfer recovery (LTR) controller that is highly robust in compensating for model discrepancies. Motter et al.[13] put forward a predictive, multiple model control strategy for the NASA Langley 16-foot tunnel based on self-organizing map, which clustered the wind tunnel dynamics and provided the Mach number by local linear modeling for candidate control inputs.

However, those methods are unsuitable for an intermittent transonic wind tunnel in China Aerodynamics Research and Development Center (CARDC) due to different control targets, wind tunnel structures and characters of the flow field. This wind tunnel cannot meet the assumed conditions in Refs.[3, 12-13] and the methods proposed in Ref.[2] cannot be employed to regulate this wind tunnel due to different control targets. This wind tunnel is required to have the control precision of Mach number of 0.001, especially for designing the large planes.

This paper focuses on realizing high-precision results in intermittent transonic wind tunnel flow field which include the following contributions:

(1) We design a novel wind tunnel control system architecture that introduces ejection pressure to mitigate the significant time lag between stagnation pressure and the main pressure regulating valve. Additionally, to address the nonlinear relationship between Mach number and static pressure, we select static pressure as a controlled variable instead of Mach number.

(2) The multi-input multi-output (MIMO) dynamic matrix controller (DMC) with the feedforward of the angle of attack is used to regulate the flow field and improve the ability of the wind tunnel to resist disturbance. The related controller parameters are discussed and selected based on first-order models and previous experience.

(3) The real wind tunnel experiments are carried out to compare the proportional integral derivative (PID) controller, the simple DMC and the proposed controller, and verify the validity and repeatability of the controller.

The rest of this paper is arranged as follows. Section 1 describes the researched wind tunnel, the control problem, and the process model of the wind tunnel. Section 2 introduces the original control system structure and an improved system. Section 3 describes the proposed MIMO DMC with the feedforward after introducing the traditional dynamic matrix controller and the MIMO dynamic matrix controller. In Section 4, practical experiment environment, the DMC tuning strategy, and experimental results are provided. The conclusions of this article are presented in Section 5.

1 Description

1.1 Intermittent transonic wind tunnel

In this wind tunnel, the Mach number, the stagnation pressure and the static pressure specify the experimental conditions and should be constant throughout a series of measurements while the angle of attack varies. However, changing the angle of attack influences the Mach number and the stagnation

pressure. The variation in the Mach number would be as high as 0.01 without control. However, wind tunnel tests require the variation of Mach number within 0.001 over the range of the angle of attack. Due to the lack of an accurate aerodynamic model, a well-tuned PID controller[14] is implemented large number on a large number of experiments. This is used for relatively slow changes of the angle of attack. The control precision of Mach number can only be within 0.003—0.004. Furthermore, in order to improve the efficiency of the wind tunnel, the rate of change of the angle of attack must be increased, which will cause a larger deviation of the Mach number.

The main body of the wind tunnel is a pressure shell (Fig.1). Evacuation is used to achieve high Mach numbers with limited power. In contrast, pressurization increases the Reynolds number, thereby reducing the influence of model factors on the measurements.

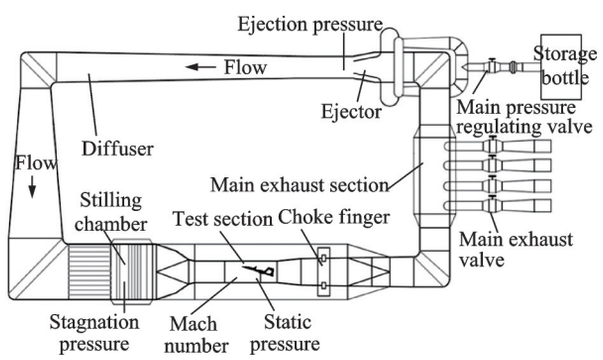

Fig.1 Schematic of temporary punching ejection type transonic wind tunnel

The wind tunnel is driven by a storage bottle with an air compressor unit. The main pressure regulating valve is used to ensure that the gas entering the wind tunnel forms the air flow in the tunnel. After leaving the ejector, the air passes two corners, expanding and flowing in the settling chamber. Then the potential energy of the air is translated to kinetic energy by a contraction section before it reaches the test section. In the test section, the scale model which should be tested is mounted. Most of the gas continues to circle in the tunnel, while the rest is exhausted through the main exhaust valve. The choke finger in the test section and the main exhaust valve in the exhaust section are employed to guarantee a uniform Mach distribution in the test section at transonic speeds.

1.2 Control problem

The model angle of attack will change according to test requirements after the stable flowing field is established, leading to the stagnation pressure and Mach number deviateing from set points. It is important to keep the Mach number constant at a predefined set point because most measured aerodynamic variables are a function of Mach number, for the given test conditions of static pressure and temperature[3,13,15]. The Mach number is influenced by many factors, but the pressure drop in the test section caused by the varying angle of attack is the most significant. During measurements, the Mach number and the stagnation pressure are needed to be controlled. In order to ensure the Mach number and the stagnation pressure constant, a PID controller is designed. The major disadvantage of the PID controller is that only small speeds of the angle of attack can be used without violating the accuracy requirement for the Mach number. For improving efficiency, it is desirable to increase the speed of the angle of attack. This speed can be adjusted between 1 (°)/s and 2 (°)/s.

Therefore, how to design a control structure and method for high-speed changing angle of attack tests is the control problem which should be solved urgently.

1.3 Process model

The physical model of the wind tunnel is complicated and in high-order, while for developing a controller, a simple low-order model is shown as

$$\frac{y_r(p)}{u_s(p)}=\frac{K_{rs}e^{-\theta_{rs}p}}{\tau_{rs}p+1} \tag{1}$$

where $y_r(p)$ is the system output; $u_s(p)$ the system input; K_{rs} the process gain; τ_{rs} the time constant; θ_{rs} the dead time; and p the Laplace operator.

To construct this model, we apply step inputs

at various set points to both the main exhaust valve and the choke finger. Subsequently, we use curve fitting to derive transfer functions for the displacements of these actuators as functions of the stagnation and static pressures. It has been shown in Ref.[16] that this complicated process can be represented, reasonably and approximatively, by a simple first-order model with time delay. The parameters K_{rs}, τ_{rs} and θ_{rs} depending on the Mach number are shown in Table 1.

Table 1 Parameters of the wind tunnel models at different Mach numbers

Controlled variable(y)	Mach number	Control signal(u)	K_{rs}	τ_{rs}	θ_{rs}
Stagnation pressure (p_0)	0.578	Displacement of the main exhaust valve	−0.014 8	1.374 2	0.702 0
	0.714		−0.054 3	1.968 2	0.559 4
	0.822		−0.059 5	2.252 8	0.528 3
	0.578	Displacement of choker finger	0.001 6	1.875 2	2.834 6
	0.714		0.003 5	2.103 7	2.542 7
	0.822		0.003 7	2.976 3	2.702 3
Static pressure (p_s)	0.578	Displacement of the main exhaust valve	−0.014 9	1.575 5	0.843 0
	0.714		−0.041 2	2.787 9	0.985 0
	0.822		−0.040 3	3.682 3	1.269 5
	0.578	Displacement of choker finger	0.030 7	1.696 2	0.832 0
	0.714		0.069 6	1.732 1	0.704 8
	0.822		0.101 5	2.985 4	0.861 4

2 Structure of the Control System

The flow field in the tunnel is regulated by three actuators, the main pressure regulating valve, the exhaust valve, and the chock finger. The stagnation pressure and the Mach number are the controlled variables in the flow field, while the air source pressure and the attack angle of scale model are considered as disturbances. The wind tunnel is a typical three-input two-output system.

The structure of wind tunnel control system is shown in Fig.2 and the generalized wind tunnel flow field is in the dashed box.

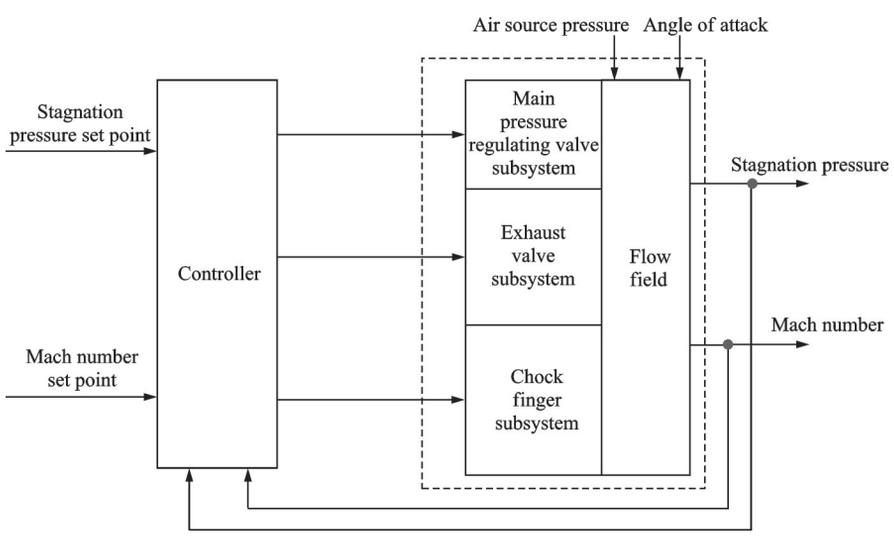

Fig.2 Structure of the wind tunnel control system

The reduction of the air source pressure during the test experiment is the main factor of time varying. The main pressure regulating valve fills the high pressure gas to the wind tunnel body and ejects

the air forming annular flow. Based on the distance between the main pressure regulating valve and test section of tunnel (about 100 m), there will be a large lag when the stagnation pressure is regulated using the main pressure regulating valve directly. Therefore, another controlled variable, the ejection pressure, is introduced. The control function is divided into two parts:

(1) The ejection pressure control, the main pressure regulating valve is used to control the ejector pressure, which is a single-input single-output system for maintaining the ejector pressure constant.

(2) The flow field control, the main exhaust valve and the choke finger are employed to control the stagnation pressure and the Mach number, which is a two-input two-output system to realize high precision control of the flow field.

According to the subsonic one dimensional isentropic flow theory, the air velocity expressed in Mach number (Ma) is calculated from the stagnation pressure (p_0) and the static pressure(p_S) in the test section[11]

$$Ma = \sqrt{5\left[\left(\frac{p_0}{p_S}\right)^{\frac{2}{7}} - 1\right]} \tag{2}$$

Considering the nonlinearity between the Mach number and the static pressure, the static pressure, instead of the Mach number, and the stagnation pressure are selected as the controlled variables which express the flow field in the test section of the wind tunnel. The flow field can be regulated by designing the controllers of the stagnation pressure and the static pressure. The restructured schematic of the wind tunnel control system is shown in Fig.3.

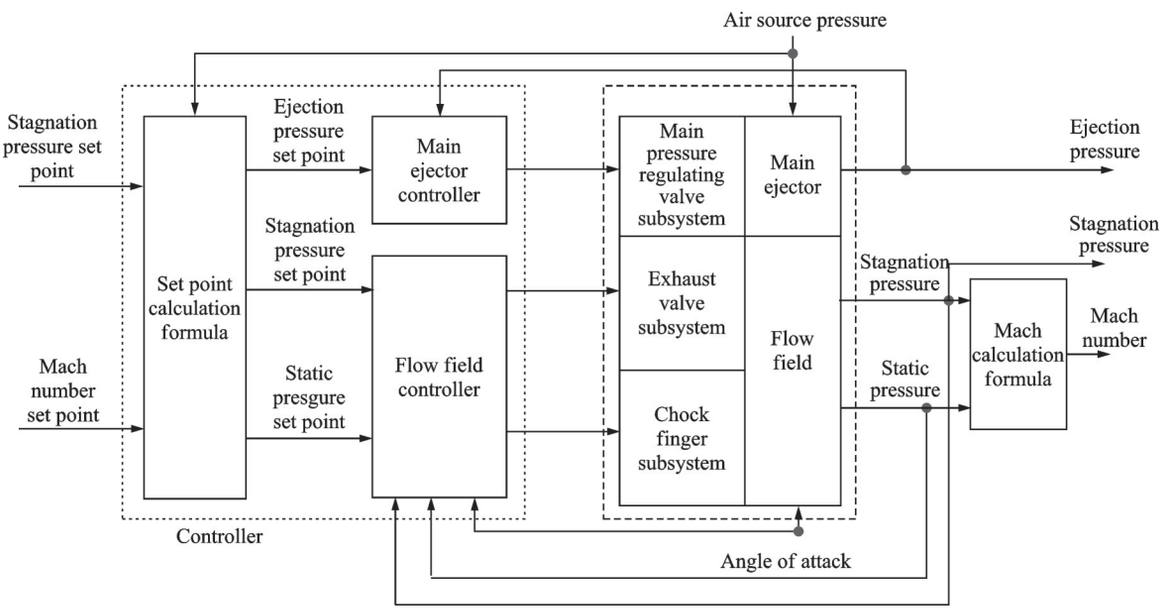

Fig.3 Restructured schematic of the wind tunnel control system

The generalized controller of the wind tunnel, which is described as the dotted box in Fig.3, consists of the set point formula, the main ejector and the flow field controller. The ejection pressure set point and the static pressure set point can be easily calculated by the subsonic one dimensional isentropic flow theory. The main concern in this wind tunnel is how to improve the flow field controller for the high precision requirements.

3 Predictive Control

The dynamic matrix controller is based on the predictive control concept that is introduced in the late seventies[17-18]. Predictive controllers are based on prediction of the future behavior of the process to be controlled. These predictions are based on a model of the process that is assumed to be available. Many papers have shown that not only "simple" processes (e.g., first without time delay) but also "dif-

ficult" processes (e.g., processes with a large time delay, non-minimum phase and unstable processes) can be controlled by predictive controllers[19-20]. Moreover, predictive controllers have shown strong robustness with respect to model mismatch.

Fig.4 indicates the way predictive controllers operate for a single-input single-output system. Suppose the current time is $t=k$, $u(k)$, $y(k)$, and $w(k)$ denote the controller output, the process output, and the desired process output at $t=k$, respectively.

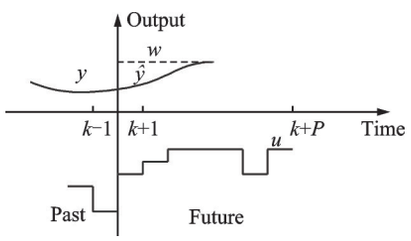

Fig.4 Predictive control concept

Further, define $\boldsymbol{u}=[u(k),u(k+1),\cdots,u(k+P-1)]^{\mathrm{T}}$, $\hat{\boldsymbol{y}}=[\hat{y}(k+1),\hat{y}(k+2),\cdots,\hat{y}(k+P)]^{\mathrm{T}}$, $\boldsymbol{w}=[w(k+1),w(k+2)\cdots,w(k+P)]^{\mathrm{T}}$, where P is the prediction horizon and the symbol "^" the prediction. The function of a predictive controller is to calculate such a future controller output sequence $\boldsymbol{u}$ that can ensure the predicted output of the process $\hat{\boldsymbol{y}}$ accurately follows the desired process output $\boldsymbol{w}$. This desired process output is often called the reference trajectory and it can be set according to process requirements. The first element of the controller output sequence $u(k)$ determined in this way is used to control the process. At the next sample time, the whole procedure is repeated by optimizing the latest measured information, which is called the receding horizon principle.

Predictive controllers are especially suitable for controlling processes with time delay. It can integrate process information subject to control and disturbance information, and this advantage leads us to select this control strategy.

3.1 Dynamic matrix controller

DMC is a widely used industrial model predictive control (MPC) method dependent on plants' step responses which was developed in the early 1970s and is a practical control system design, particularly in the oil and petrochemical industries[21-23]. In this section, single-input single-output (SISO) formulation of the DMC is briefly reviewed.

In the wind tunnel, the flow field is a typical open loop stable plant with relatively slow and simple dynamics. For such plants, the finite step response (FSR) models are adequate. FSR models which are readily employed by DMC can sufficiently capture the plant dynamics[24-25]. Assume that $y(t)$ is the controlled variable, $\Delta u(t)=u(t)-u(t-1)$ is the control signal and is the control increment. Then, the system step response can be described as

$$y(t)=\sum_{i=1}^{\infty}a_i\Delta u(t-i) \tag{3}$$

where a_i is the sampled step responses. Let $\hat{f}(t)$ be the disturbance, then the predicted values will be described as(starting predictions from instant t)

$$\begin{aligned}(t+k|t)=&\sum_{i=1}^{\infty}a_i\Delta u(t+k-i)+\hat{f}(t+k)=\\&\sum_{i=1}^{k}a_i\Delta u(t+k-i)+\\&\sum_{i=k+1}^{\infty}a_i\Delta u(t+k-i)+\hat{f}(t+k)\end{aligned} \tag{4}$$

Considering constant disturbances, $y_{\mathrm{m}}(t)$ is the measured output value.

$$\hat{f}(t+k)=\hat{f}(t)=y_{\mathrm{m}}(t)-\sum_{i=1}^{\infty}a_i\Delta u(t-i) \tag{5}$$

Then

$$\begin{aligned}\hat{y}(t+k|t)=&\sum_{i=1}^{k}a_i\Delta u(t+k-i)+\\&\sum_{i=k+1}^{\infty}a_i\Delta u(t+k-i)+y_{\mathrm{m}}(t)-\\&\sum_{i=1}^{\infty}a_i\Delta u(t-i)\end{aligned} \tag{6}$$

Rewrite the second item as

$$\sum_{i=k+1}^{\infty}a_i\Delta u(t+k-i)=\sum_{i=1}^{\infty}a_{k+i}\Delta u(t-i) \tag{7}$$

Then

$$\begin{aligned}\hat{y}(t+k|t)=&\sum_{i=1}^{k}a_i\Delta u(t+k-i)+y_{\mathrm{m}}(t)+\\&\sum_{i=1}^{\infty}(a_{k+i}-a_i)\Delta u(t-i)\end{aligned} \tag{8}$$

If the process is asymptotically stable, coefficients of step response a_i will tend to be a constant value after sample periods, so

$$a_{k+i}-a_i\approx 0 \quad i>N \tag{9}$$

The output prediction values along the finite horizon will be

$$\hat{\boldsymbol{y}}=\begin{bmatrix}\hat{y}(t+1|t)\\ \hat{y}(t+2|t)\\ \vdots\\ \hat{y}(t+P|t)\end{bmatrix}_{P\times 1},\quad \Delta\boldsymbol{u}=\begin{bmatrix}\Delta u(t)\\ \Delta u(t+1)\\ \vdots\\ \Delta u(t+M-1)\end{bmatrix}_{M\times 1},\quad \Delta\boldsymbol{u}_{\text{past}}=\begin{bmatrix}\Delta u(t-1)\\ \Delta u(t-2)\\ \vdots\\ \Delta u(t-N)\end{bmatrix}_{N\times 1},\quad \boldsymbol{y}_{\text{m}}=\begin{bmatrix}y_{\text{m1}}(t)\\ y_{\text{m1}}(t)\\ \vdots\\ y_{\text{m1}}(t)\end{bmatrix}_{P\times 1} \tag{12a}$$

$$\boldsymbol{A}=\begin{bmatrix}a_1 & 0 & \cdots & 0 & 0\\ a_2 & a_1 & \cdots & 0 & 0\\ \vdots & \vdots & & \vdots & \vdots\\ a_{M-1} & a_{M-2} & \cdots & a_1 & 0\\ a_M & a_{M-1} & \cdots & a_2 & a_1\\ a_{M+1} & a_M & \cdots & a_3 & a_2\\ \vdots & \vdots & & \vdots & \vdots\\ a_{P-1} & a_{P-2} & \cdots & a_{P-M+1} & a_{P-M}\\ a_P & a_{P-1} & \cdots & a_{P-M+2} & a_{P-M+1}\end{bmatrix}_{P\times M},\quad \boldsymbol{B}=\begin{bmatrix}a_2-a_1 & a_3-a_2 & \cdots & a_{N+1}-a_N\\ a_3-a_1 & a_4-a_2 & \cdots & a_{N+2}-a_N\\ \vdots & \vdots & & \vdots\\ a_P-a_1 & a_{P+1}-a_2 & \cdots & a_{P+N-1}-a_N\\ a_{P+1}-a_1 & a_{P+2}-a_2 & \cdots & a_{P+N}-a_N\end{bmatrix}_{P\times N} \tag{12b}$$

where M is the control horizon ($M\leqslant P$); $\boldsymbol{A}$ the dynamic matrix. The quadratic objective index in the DMC structure is

$$J=\sum_{j=1}^{P}\left[\hat{y}(t+j)-w(t+j)\right]^2+\sum_{j=1}^{M}\lambda^2\left[\Delta u(t+j-1)\right]^2 \tag{13}$$

where λ^2 is the move suppression coefficient, which is an important tuning parameter in DMC.

The vector form of the quadratic objective index is

$$J=(\hat{\boldsymbol{y}}-\boldsymbol{w})^{\mathrm{T}}(\hat{\boldsymbol{y}}-\boldsymbol{w})+\lambda^2\Delta\boldsymbol{u}^{\mathrm{T}}\Delta\boldsymbol{u} \tag{14}$$

$$\boldsymbol{w}=\begin{bmatrix}w(t+1)\\ w(t+2)\\ \vdots\\ w(t+P)\end{bmatrix}_{P\times 1} \tag{15}$$

In a problem without constraints, the optimized control efforts vector is obtained by solving

$$\frac{\mathrm{d}J}{\mathrm{d}\Delta\boldsymbol{u}}=0 \tag{16}$$

The control signal is calculated as

$$\boldsymbol{u}=(\boldsymbol{A}^{\mathrm{T}}\boldsymbol{A}+\lambda\boldsymbol{I})^{-1}\boldsymbol{A}^{\mathrm{T}}(\boldsymbol{w}-\boldsymbol{B}\Delta\boldsymbol{u}_{\text{past}}-\boldsymbol{y}_{\text{m}}) \tag{17}$$

Consequently, the SISO DMC tuning parameters can be listed as λ^2, P, N, M and T, where T is the sampling time.

$$\hat{y}(t+k|t)=\sum_{i=1}^{k}a_i\Delta u(t+k-i)+\sum_{i=1}^{N}(a_{k+i}-a_i)\Delta u(t-i)+y_{\text{m}}(t) \tag{10}$$

In the vector form we have

$$\hat{\boldsymbol{y}}=\boldsymbol{A}\Delta\boldsymbol{u}+\boldsymbol{B}\Delta\boldsymbol{u}_{\text{past}}+\boldsymbol{y}_{\text{m}} \tag{11}$$

3.2 MIMO dynamic matrix controller

The SISO DMC can be easily extended in multivariable systems by a set of linear difference equations[26-27]. For a $S\times R$ MIMO system (S inputs, R outputs) like the intermittent transonic wind tunnel, outputs of a $S\times R$ system using its step response model can be represented as

$$\hat{y}_r(t+k|t)=\sum_{s=1}^{S}\sum_{i=1}^{k}a_i^{s,r}\Delta u_s(t+k-i)+y_{\text{mr}}(t)+\sum_{s=1}^{S}\sum_{i=1}^{N}(a_{k+i}^{s,r}-a_i^{s,r})\Delta u_s(t-i)$$
$$r=1,2,\cdots,R \tag{18}$$

where u_s and Δu_s are the sth input and its increment, respectively; $a_k^{s,r}$ is the step response coefficients obtained by the sth input acting on the rth thoutput at sample time k and N the sample time at which the step response reaches steady state.

The future predictions of the system outputs for the P based on the M, can be written as

$$\hat{\boldsymbol{y}}=\boldsymbol{A}\Delta\boldsymbol{u}+\boldsymbol{B}\Delta\boldsymbol{u}_{\text{past}}+\boldsymbol{y}_{\text{m}} \tag{19}$$

$$\hat{\boldsymbol{y}}=\begin{bmatrix}\hat{y}_1(t+1)\\ \hat{y}_1(t+2)\\ \vdots\\ \hat{y}_1(t+P)\\ \hat{y}_2(t+1)\\ \hat{y}_2(t+2)\\ \vdots\\ \hat{y}_{R-1}(t+P)\\ \hat{y}_R(t+1)\\ \vdots\\ \hat{y}_R(t+P-1)\\ \hat{y}_R(t+P)\end{bmatrix}_{RP\times 1},\quad \Delta\boldsymbol{u}=\begin{bmatrix}\Delta u_1(t)\\ \Delta u_1(t+1)\\ \vdots\\ \Delta u_1(t+M-1)\\ \Delta u_2(t)\\ \Delta u_2(t+1)\\ \vdots\\ \Delta u_{S-1}(t+M-1\\ \Delta u_S(t)\\ \vdots\\ \Delta u_S(t+M-2)\\ \Delta u_S(t+M-1)\end{bmatrix}_{SM\times 1},\quad \Delta\boldsymbol{u}_{\text{past}}=\begin{bmatrix}\Delta u_1(t-1)\\ \Delta u_1(t-2)\\ \vdots\\ \Delta u_1(t-N)\\ \Delta u_2(t-1)\\ \Delta u_2(t-2)\\ \vdots\\ \Delta u_{S-1}(t-N)\\ \Delta u_S(t-1)\\ \vdots\\ \Delta u_S(t-N+1)\\ \Delta u_S(t-N)\end{bmatrix}_{SN\times 1} \tag{20a}$$

$$\boldsymbol{y}_{\text{m}}=\begin{bmatrix}y_{\text{m}1}(t+1)\\ y_{\text{m}1}(t+2)\\ \vdots\\ y_{\text{m}1}(t+P)\\ y_{\text{m}2}(t+1)\\ y_{\text{m}2}(t+2)\\ \vdots\\ y_{\text{m}(R-1)}(t+P)\\ y_{\text{m}R}(t+1)\\ \vdots\\ y_{\text{m}R}(t+P-1)\\ y_{\text{m}R}(t+P)\end{bmatrix}_{RP\times 1},\quad \boldsymbol{A}=\begin{bmatrix}\boldsymbol{A}_{1,1} & \boldsymbol{A}_{2,1} & \cdots & \boldsymbol{A}_{S,1}\\ \boldsymbol{A}_{1,2} & \boldsymbol{A}_{2,2} & \cdots & \boldsymbol{A}_{S,2}\\ \vdots & \vdots & & \vdots\\ \boldsymbol{A}_{1,R-1} & \boldsymbol{A}_{2,R-1} & \cdots & \boldsymbol{A}_{S,R-1}\\ \boldsymbol{A}_{1,R} & \boldsymbol{A}_{2,R} & \cdots & \boldsymbol{A}_{S,R}\end{bmatrix},\quad \boldsymbol{A}_{m,n}=\begin{bmatrix}a_1^{m,n} & 0 & 0 & \cdots & 0\\ a_2^{m,n} & a_1^{m,n} & 0 & \cdots & 0\\ \vdots & \vdots & \vdots & & \vdots\\ a_M^{m,n} & a_{M-1}^{m,n} & a_{M-2}^{m,n} & \cdots & a_1^{m,n}\\ \vdots & \vdots & \vdots & & \vdots\\ a_P^{m,n} & a_{P-1}^{m,n} & a_{P-2}^{m,n} & \cdots & a_{P-M+1}^{m,n}\end{bmatrix}_{P\times M} \tag{20b}$$

$$\boldsymbol{B}=\begin{bmatrix}a_2^{1,1}-a_1^{1,1} & a_3^{1,1}-a_2^{1,1} & \cdots & a_{N+1}^{1,1}-a_N^{1,1} & a_2^{2,1}-a_1^{2,1} & a_3^{2,1}-a_2^{2,1} & \cdots & a_{N+1}^{2,1}-a_N^{2,1} & \cdots & a_{N+1}^{S,1}-a_N^{S,1}\\ a_3^{1,1}-a_1^{1,1} & a_4^{1,1}-a_2^{1,1} & \cdots & a_{N+2}^{1,1}-a_N^{1,1} & a_3^{2,1}-a_1^{2,1} & a_4^{2,1}-a_2^{2,1} & \cdots & a_{N+2}^{2,1}-a_N^{2,1} & \cdots & a_{N+2}^{S,1}-a_N^{S,1}\\ \vdots & \vdots & & \vdots & \vdots & \vdots & & \vdots & & \vdots\\ a_{P+1}^{1,1}-a_1^{1,1} & a_{P+2}^{1,1}-a_2^{1,1} & \cdots & a_{N+P}^{1,1}-a_N^{1,1} & a_{P+1}^{2,1}-a_1^{2,1} & a_{P+2}^{2,1}-a_2^{2,1} & \cdots & a_{N+P}^{2,1}-a_N^{2,1} & \cdots & a_{N+P}^{S,1}-a_N^{S,1}\\ a_2^{1,2}-a_1^{1,2} & a_3^{1,2}-a_2^{1,2} & \cdots & a_{N+1}^{1,2}-a_N^{1,2} & a_2^{2,2}-a_1^{2,2} & a_3^{2,2}-a_2^{2,2} & \cdots & a_{N+1}^{2,2}-a_N^{2,2} & \cdots & a_{N+1}^{S,2}-a_N^{S,2}\\ \vdots & \vdots & & \vdots & \vdots & \vdots & & \vdots & & \vdots\\ a_{P+1}^{1,R}-a_1^{1,R} & a_{P+2}^{1,R}-a_2^{1,R} & \cdots & a_{N+P}^{1,R}-a_N^{1,R} & a_{P+1}^{2,R}-a_1^{2,R} & a_{P+1}^{2,R}-a_2^{2,R} & \cdots & a_{P+N}^{2,R}-a_N^{2,R} & \cdots & a_{P+N}^{S,R}-a_N^{S,R}\end{bmatrix}_{RP\times SN} \tag{20c}$$

The future control increment $\Delta\boldsymbol{u}$ is determined according to the solution of the following optimization problem.

$$\min_{\Delta\boldsymbol{u}} J=(\boldsymbol{w}-\hat{\boldsymbol{y}})^{\mathrm{T}}\boldsymbol{\Gamma}^{\mathrm{T}}\boldsymbol{\Gamma}(\boldsymbol{w}-\hat{\boldsymbol{y}})+\Delta\boldsymbol{u}^{\mathrm{T}}\boldsymbol{\Lambda}^{\mathrm{T}}\boldsymbol{\Lambda}\Delta\boldsymbol{u} \tag{21}$$

where $\boldsymbol{\Gamma}$ and $\boldsymbol{\Lambda}$ are weighting matrices on prediction errors and control effort, respectively. Considering unconstraint minimization, the optimal control signal is determined as

$$\Delta\boldsymbol{u}=(\boldsymbol{A}^{\mathrm{T}}\boldsymbol{\Gamma}^{\mathrm{T}}\boldsymbol{\Gamma}\boldsymbol{A}+\boldsymbol{\Lambda}^{\mathrm{T}}\boldsymbol{\Lambda})^{-1}\boldsymbol{A}^{\mathrm{T}}\boldsymbol{\Gamma}^{\mathrm{T}}\boldsymbol{\Gamma}(\boldsymbol{w}-\boldsymbol{B}\Delta\boldsymbol{u}_{\text{past}}-\boldsymbol{y}_{\text{m}}) \tag{22}$$

The first component of $\Delta\boldsymbol{u}$ is usually applied to

the system. This procedure is performed in each sampling interval. The matrix of controlled variable weights $\boldsymbol{\Gamma}^{\mathrm{T}}\boldsymbol{\Gamma}$ has $\gamma_r^2(r=1,2,\cdots,R)$ as the leading diagonal elements of the rth diagonal matrix block

$$\boldsymbol{\Gamma}^{\mathrm{T}}\boldsymbol{\Gamma}=\begin{bmatrix}\gamma_1^2 I_{P\times P} & 0 & 0\\ 0 & \ddots & 0\\ 0 & 0 & \gamma_R^2 I_{P\times P}\end{bmatrix}_{RP\times RP}$$

The matrix of move suppression coefficients $\boldsymbol{\Lambda}^{\mathrm{T}}\boldsymbol{\Lambda}$ has $\lambda_s^2(s=1,2,\cdots,S)$ as the leading diagonal elements of the sth diagonal matrix block, or

$$\boldsymbol{\Lambda}^{\mathrm{T}}\boldsymbol{\Lambda}=\begin{bmatrix}\lambda_1^2 I_{M\times M} & 0 & 0\\ 0 & \ddots & 0\\ 0 & 0 & \lambda_S^2 I_{M\times M}\end{bmatrix}_{SM\times SM}$$

3.3 Feedforward in DMC

In wind tunnel tests, the angle of attack is usually changed with a fixed 4° step with a speed of 2(°)/s from −4° to 10°. After a stable flow field has been established, with the displacement of the main exhaust valve and the choke finger held constant, a 4° step change in the angle of attack is applied to determine its influence on the stagnation and static pressures. Figs.5(a, b) are the step response of attack angle acting on the static pressure and the stagnation pressure, at a step from 4° to 8° of $Ma=0.578$, respectively.

For a "general tested model", the maximum sensitivity of the Mach number to the angle of attack is about 0.002 Mach/(°). In Fig.5, changing the angle of attack has little effect on the stagnation pressure, while this change causes the static pressure increasing. Meanwhile, as shown in Fig.5, the effect of the angle of attack on the static pressure can approximate to adding a first order plus time dead item to the static pressure.

The traditional DMC is on the premise that the disturbances' effect on the system outputs is unclear. However, in wind tunnel tests, the main disturbance which is caused by the change of angle of attack is predictable. Since feedforward control is

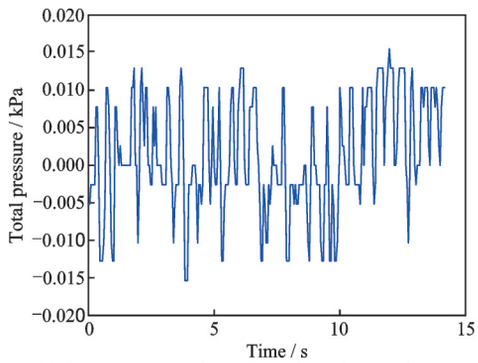

(a) Step response of attack angle acting on the stagnation pressure when Ma=0.578

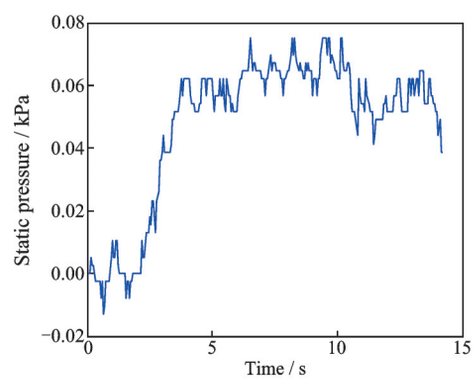

(b) Step response of attack angle acting on the static pressure when Ma=0.578

Fig.5 Step response of attack angle acting on the stagnation pressure and the static pressure at $Ma=0.578$

pretty effective to cope with predictable disturbances, it is reasonable to combine feedforward and DMC to accelerate the process of resisting the disturbance[28].

The predicted outputs of DMC compensated by disturbances can be reconstructed as

$$\begin{aligned}\hat{y}_r(t+k|t)=&\sum_{s=1}^{S}\sum_{i=1}^{k}a_i^{s,r}\Delta u_s(t+k-i)+y_{\mathrm{m}r}(t)+\\&\sum_{s=1}^{S}\sum_{i=1}^{N}(a_{k+i}^{s,r}-a_i^{s,r})\Delta u_s(t-i)+\\&\sum_{o=1}^{O}\sum_{i=1}^{k}c_i^{o,r}\Delta v_o(t+k-i)+\\&\sum_{o=1}^{O}\sum_{i=1}^{Q}(c_{i+1}^{o,r}-c_i^{o,r}a_i^{s,r})\Delta v_o(t-i)\\ r=1,2,\cdots,R\end{aligned}\tag{23}$$

where Δv_o is the disturbance variation, $\Delta v_o(t)=v_o(t)-v_o(t-1)$. The predicted outputs in vector form are

$$\hat{\boldsymbol{y}}=\boldsymbol{A}\Delta\boldsymbol{u}+\boldsymbol{B}\Delta\boldsymbol{u}_{\mathrm{past}}+\boldsymbol{C}\Delta\boldsymbol{v}+\boldsymbol{D}\Delta\boldsymbol{v}_{\mathrm{past}}+\boldsymbol{y}_{\mathrm{m}}\tag{24}$$

$$\Delta \boldsymbol{v}=\begin{bmatrix}\Delta v_1(t)\\ \Delta v_1(t+1)\\ \vdots\\ \Delta v_1(t+P-1)\\ \Delta v_2(t)\\ \Delta v_2(t+1)\\ \vdots\\ \Delta v_{O-1}(t+P-1)\\ \Delta v_O(t)\\ \vdots\\ \Delta v_O(t+P-2)\\ \Delta v_O(t+P-1)\end{bmatrix}_{OP\times 1},\quad \Delta \boldsymbol{v}_{\text{past}}=\begin{bmatrix}\Delta v_1(t-1)\\ \Delta v_1(t-2)\\ \vdots\\ \Delta v_1(t-Q)\\ \Delta v_2(t-1)\\ \Delta v_2(t-2)\\ \vdots\\ \Delta v_{O-1}(t-Q)\\ \Delta v_O(t-1)\\ \vdots\\ \Delta v_O(t-Q+1)\\ \Delta v_O(t-Q)\end{bmatrix}_{OQ\times 1} \tag{25a}$$

$$\boldsymbol{C}=\begin{bmatrix}\boldsymbol{C}_{1,1} & \boldsymbol{C}_{2,1} & \cdots & \boldsymbol{C}_{O,1}\\ \boldsymbol{C}_{1,2} & \boldsymbol{C}_{2,2} & \cdots & \boldsymbol{C}_{O,2}\\ \vdots & \vdots & & \vdots\\ \boldsymbol{C}_{1,R} & \boldsymbol{C}_{2,R} & \cdots & \boldsymbol{C}_{O,R}\end{bmatrix}_{RP\times OP},\quad \boldsymbol{C}_{o,r}=\begin{bmatrix}c_1^{o,r} & 0 & 0 & \cdots & 0\\ c_2^{o,r} & c_1^{o,r} & 0 & \cdots & 0\\ \vdots & \vdots & \vdots & & \vdots\\ c_P^{o,r} & c_{P-1}^{o,r} & c_{P-2}^{o,r} & \cdots & c_1^{o,r}\end{bmatrix}_{P\times P} \tag{25b}$$

$$\boldsymbol{D}=\begin{bmatrix}c_2^{1,1}-c_1^{1,1} & c_3^{1,1}-c_2^{1,1} & \cdots & c_{Q+1}^{1,1}-c_Q^{1,1} & c_2^{2,1}-c_1^{2,1} & c_3^{2,1}-c_2^{2,1} & \cdots & c_{Q+1}^{2,1}-c_Q^{2,2} & \cdots & c_{Q+1}^{O,1}-c_Q^{O,1}\\ c_3^{1,1}-c_1^{1,1} & c_4^{1,1}-c_2^{1,1} & \cdots & c_{Q+2}^{1,1}-c_Q^{1,1} & c_3^{2,1}-c_1^{2,1} & c_4^{2,1}-c_2^{2,1} & \cdots & c_{Q+2}^{2,1}-c_Q^{2,1} & \cdots & c_{Q+2}^{O,1}-c_Q^{O,1}\\ \vdots & \vdots & & \vdots & \vdots & \vdots & & \vdots & & \vdots\\ c_{P+1}^{1,1}-c_1^{1,1} & c_{P+2}^{1,1}-c_2^{1,1} & \cdots & c_{Q+P}^{1,1}-c_Q^{1,1} & c_{P+1}^{2,1}-c_1^{2,1} & c_{P+2}^{2,1}-c_2^{2,1} & \cdots & c_{Q+P}^{2,1}-c_Q^{2,1} & \cdots & c_{Q+P}^{O,1}-c_Q^{O,1}\\ c_2^{1,2}-c_1^{1,2} & c_3^{1,2}-c_2^{1,2} & \cdots & c_{Q+1}^{1,2}-c_Q^{1,2} & c_2^{2,2}-c_1^{2,2} & c_3^{2,2}-c_2^{2,2} & \cdots & c_{Q+1}^{2,2}-c_Q^{2,2} & \cdots & c_{Q+1}^{O,2}-c_Q^{O,2}\\ \vdots & \vdots & & \vdots & \vdots & \vdots & & \vdots & & \vdots\\ c_{P+1}^{1,R}-c_1^{1,R} & c_{P+2}^{1,R}-c_2^{1,R} & \cdots & c_{Q+P}^{1,R}-c_Q^{1,R} & c_{P+1}^{2,R}-c_1^{2,R} & c_{P+2}^{2,R}-c_2^{2,R} & \cdots & c_{P+Q}^{2,R}-c_Q^{2,R} & \cdots & c_{P+Q}^{O,R}-c_Q^{O,R}\end{bmatrix}_{RP\times OQ} \tag{25c}$$

where $c_k^{o,r}$ is the step response coefficients obtained for the disturbance acting on the output at sample time k; Q the sample time when the step response caused by the disturbance reaches to its steady state; and O the number of disturbance sources.

In such a situation, the optimal control signal of DMC is

$$\Delta \boldsymbol{u}=(\boldsymbol{A}^{\mathrm{T}}\boldsymbol{\Gamma}^{\mathrm{T}}\boldsymbol{\Gamma}\boldsymbol{A}+\boldsymbol{\Lambda}^{\mathrm{T}}\boldsymbol{\Lambda})^{-1}\boldsymbol{A}^{\mathrm{T}}\boldsymbol{\Gamma}^{\mathrm{T}}\boldsymbol{\Gamma}(\boldsymbol{w}-B\Delta \boldsymbol{u}_{\text{past}}-C\Delta \boldsymbol{v}-D\Delta \boldsymbol{v}_{\text{past}}-\boldsymbol{y}_{\text{m}}) \tag{26}$$

4 Experiment

4.1 Experiment environment

The experiment is set up as follows.

Pressure instrument: 0.03% of scope for the stagnation pressure and the static pressure. Scale model: The scale model of plane TU154, blocking degree 1%. DMC : An industrial computer with LabVIEW system, 4 kernel CPU and 4G RAM. PID controller: A programmable logistic controller (PLC) of general electric(GE) company.

Response experiments: To obtain the step response data for the DMC, several experiments under different Mach number set points are carried out and their detailed information is shown in Table 2.

The step rules of angle of attack are in accordance with the actual test rules. Since the step responses caused by equivalent change of angle of attack in different angle regions are different, the disturbance models employed by DMC need to be

Table 2 Setup of the step response experiments

Mach number	Displacement of the main exhaust valve	Displacement of the choker finger	Angle of attack/(°)
0.578	35	40	4
0.714	30	30	4
0.822	30	20	4

changed according to the angle of attack.

4.2 DMC tuning strategy

The adjustable parameters in an unconstrained MIMO DMC that affect the closed loop performance include the sample time, the model horizon, the prediction horizon, the control horizon, the controlled variable weights and the move suppression coefficients. The tuning challenge presented by this set of adjustable parameters is important since many of the parameters have overlapping effects on closed-loop performance[29-30].

Several DMC tuning strategies are discussed in the previous literatures, but only a few provide analytical and closed form expressions for the tuning parameters which are briefly introduced. A pioneer paper in this field was completed in Ref.[31] that provided a tuning formulation on the basis of the first order plus dead time (FOPDT) model.

Although a FOPDT model approximation does not capture all the features of some higher order processes, it reasonably describes the process gain, overall time constant, and effective dead time of such processes. In the past, tuning strategies based on a FOPDT model such as Cohen-Coon, integral of absolute error (IAE), and integral of time-weighted absolute error (ITAE) have been proved useful for PID implementations. The tuning strategy presented here is significant because it offers an analogous approach for DMC[31-32].

The process of tuning parameters based on the FOPDT model is shown as follows.

(1) Approximate the process dynamics of all controller output-controlled variable pairs with FOPDT models

$$\frac{y_r(p)}{u_s(p)}=\frac{K_{rs}e^{-\theta_{rs}p}}{\tau_{rs}p+1} \quad r=1,2;s=1,2 \tag{27}$$

The FOPDT time models of the intermittent transonic wind tunnel are built and the model parameters are shown in Table 1.

(2) Select the sample time, which should meet the following conditions

$$T\leqslant \mathrm{Min}(T_{rs}),\quad T_{rs}=\mathrm{Max}(0.1\tau_{rs},0.5\theta_{rs}) \tag{28}$$

According to Eq.(28), the sample time are 137 ms, 173 ms and 255 ms at Mach number 0.578, 0.714 and 0.822, respectively. For eliminating 50 Hz power frequency interference and engineering convenience, we chose 100 ms as the real sample time. Therefore, the other control parameters are selected on the basis of $T=100$ ms.

(3) Compute the P and the model horizon N

$$\begin{cases} P\geqslant \mathrm{Max}\left(\dfrac{5\tau_{rs}}{T}+k_{rs}\right) \\ k_{rs}=\dfrac{\theta_{rs}}{T}+1 \\ N\geqslant P \end{cases} \tag{29}$$

At three set Mach numbers, P are 123, 150 and 197. However, the prediction horizon selected according to Eq.(29) is pretty conservative and add some unwanted computation. In addition, a uniform prediction horizon is more applicable and convenient for practical engineering. So P is selected as 128 for easier storage allocation.

In terms of N, apart from the third item in Eq.(29), $N\times T$ should be larger than the time when controlled variables' step response becomes steady. Considering the wind tunnel step response can reach steady, N is set as 200.

(4) Select M. It is recommend that M is supposed to be larger than 63.2% of the settling time of the slowest sub-process in a multivariable system[32]. But this is too conservative and leads to overmuch computation. Actually, for simple processes, like a first-order model with time delay, $M=1$ is adequate[31].

(5) Select the γ_r^2 to scale controlled variable measurements to similar magnitudes. In the wind tunnel, the stagnation pressure and the static pressure are in the same order of magnitude, so let $\gamma_1^2=\gamma_2^2=1$.

(6) Select λ_s^2. Since the M is 1, the setpoint step response is sluggish. Under this condition, increasing λ_s^2 will only slow the process response, and no move suppression coefficients should be used ($\lambda_1^2=\lambda_2^2=0$).

Based on the above-mentioned six steps, the DMC parameters used in the intermittent transonic wind tunnel are selected, as shown in Table 3.

Table 3 Parameters of the step response experiments

T/ms	P	N	M	γ_1^2	γ_2^2	λ_1^2	λ_2^2
100	128	200	1	1	1	0	0

In order to examine the DMC, multiple flow experiments are conducted at different Mach numbers and stagnation pressure. The change rate of the attack angle is 2(°)/s and the scope of varying is from −4° to 10° in all experiments. To verify the performance of DMC, the following four criteria are used.

(1) Accuracy E, the expectation value of control error absolute value in a period. This index is expressed by the average value of control error in the period when angle of attack varies.

$$E=\frac{1}{B_2-B_1+1}\sum_{t=B_1}^{B_2}|e(t)| \tag{30}$$

where $e(t)=w(t)-y_m(t)$ is the control error at sample time t, $w(t)$ and $y_m(t)$ are the set value and the actual value of controlled variable, respectively; B_1 and B_2 are the start and the end time of changing angle of attack, respectively.

(2) Precision σ, the fluctuant degree of controlled variable, is evaluated by the standard deviation of controlled variables.

$$\sigma=\sqrt{\frac{1}{B_2-B_1}\sum_{t=B_1}^{B_2}[y_m(t)-\mu]^2} \tag{31}$$

where $\mu=\dfrac{1}{B_2-B_1+1}\sum_{t=B_1}^{B_2}y_m(t)$ is the average value of controlled variable between B_1 and B_2.

(3) Maximum positive error (MPE)

$$\mathrm{MPE}=\max[y_m(t)]-w(t) \tag{32}$$

(4) Maximum negative error (MNE)

$$\mathrm{MNE}=\min[y_m(t)]-w(t) \tag{33}$$

4.2.1 The proposed controller vs the PID controller

Table 4 compares the criteria of the proposed controller (DMC with feedforward) and the PID controller at Ma=0.578. The emor amount of stagnation pressure is denoted by TP. Because of the future prediction, the accuracy of the proposed controller is smaller than that of PID, and the precision of the proposed controller is higher. Furthermore, the MPE and the MNE of PID controller are larger than those of the proposed controller. This illustrates that the DMC with feedforward can regulate the wind tunnel better.

Table 4 Comparison between the proposed controller and the PID controller of Ma=0.578

Mode	E		σ		MPE		MNE	
	δ_{Ma}	TP/kPa	δ_{Ma}	TP/kPa	δ_{Ma}	TP/kPa	δ_{Ma}	TP/kPa
PID	0.001 5	0.140 8	0.003 0	0.076 8	0.004 5	0.333 6	−0.003 7	−0.100 6
The proposed	0.000 5	0.005 5	0.000 7	0.040 7	0.002 2	0.129 2	−0.002 0	−0.129 3

The proposed DMC outperforms PID control primarily because DMC is based on the system's dynamic model, allowing it to predict future outputs and respond to disturbances in advance, thus avoiding lag effects. Additionally, DMC is suitable for MIMD systems and achieves precise control through optimization algorithms, maintaining stability and accuracy during rapid changes in angle of attack. These advantages make DMC particularly effective in wind tunnel Mach number control tasks.

Fig.6 describes the control performance of the PID controller, while the control performance of the proposed controller is shown in Fig.7. Compared Fig.6 and Fig.7, it can be observed that the stagnation pressure and the static pressure controlled by the proposed controller track their setpoints more accurately, which is also beneficial to Mach number.

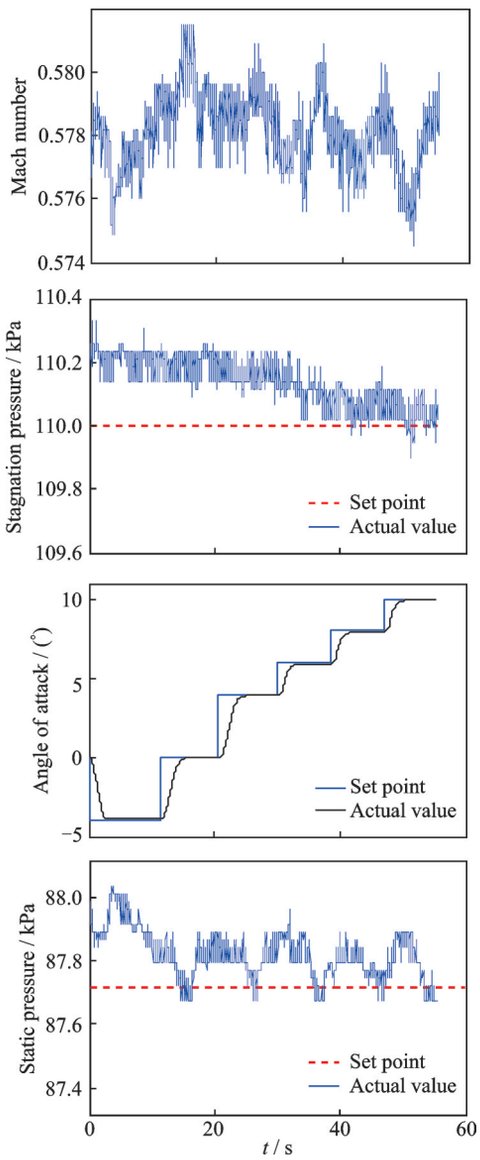

Fig.6 Control performance of PID when Ma=0.578

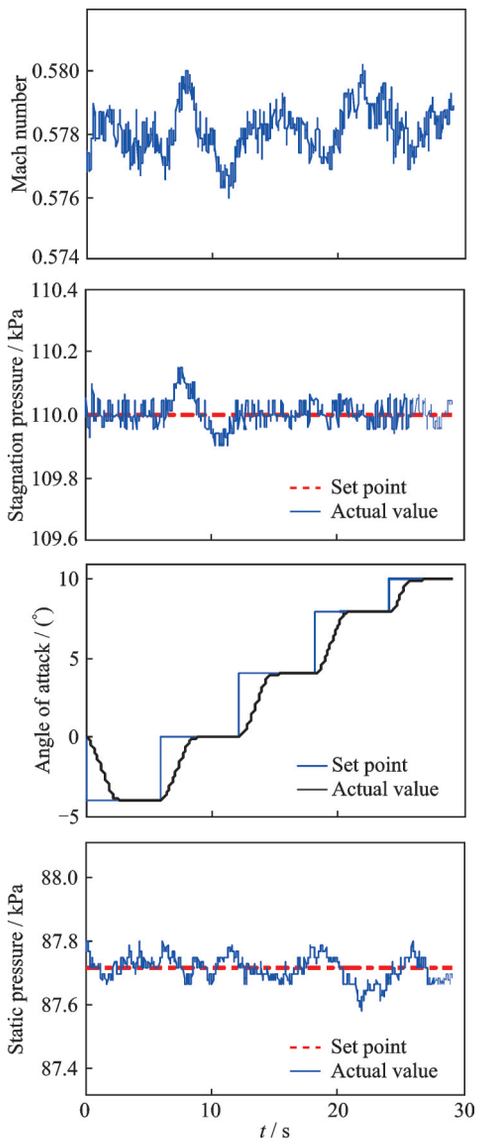

Fig.7 Control performance of the proposed controller when Ma=0.578

4.2.2 DMC vs the DMC with feedforward

To verify the performance of feedforward, two experiments are carried out under the condition when Ma=0.578 and stagnation pressure is 110 kPa. One is controlled by the simple DMC, while the other is regulated by the proposed controller (DMC with feedforward). The detailed control criteria are shown in Table 5.

Feedforward-compensated DMC performs better than DMC without feedforward compensation in wind tunnel Mach number control primarily because feedforward compensation can predict outputs in advance and adjust for disturbances, thereby reducing lag response, improving steady-state performance, lowering control bias, and enhancing the system's robustness against external disturbances. Additionally, the combination of feedforward and feedback control allow DMC to adjust control strategies more flexibly, resulting in better performance during

Table 5 Comparison between the proposed controller and the DMC of Ma=0.578

Mode	E		σ		MPE		MNE	
	δ_{Ma}	TP/kPa	δ_{Ma}	TP/kPa	δ_{Ma}	TP/kPa	δ_{Ma}	TP/kPa
DMC	0.000 8	0.006 3	0.001 3	0.065 3	0.002 9	0.243 2	−0.002 4	−0.267 1
The proposed	0.000 6	0.005 5	0.000 7	0.040 7	0.002 2	0.129 2	−0.002 0	−0.129 3

changes in the angle of attack. These factors collectively enhance the response speed and control accuracy of the feedforward-compensated DMC.

Fig.8 shows the control performance of simple DMC. Although the simple DMC has already improved control performance of the wind tunnel, the proposed controller shows better control criteria.

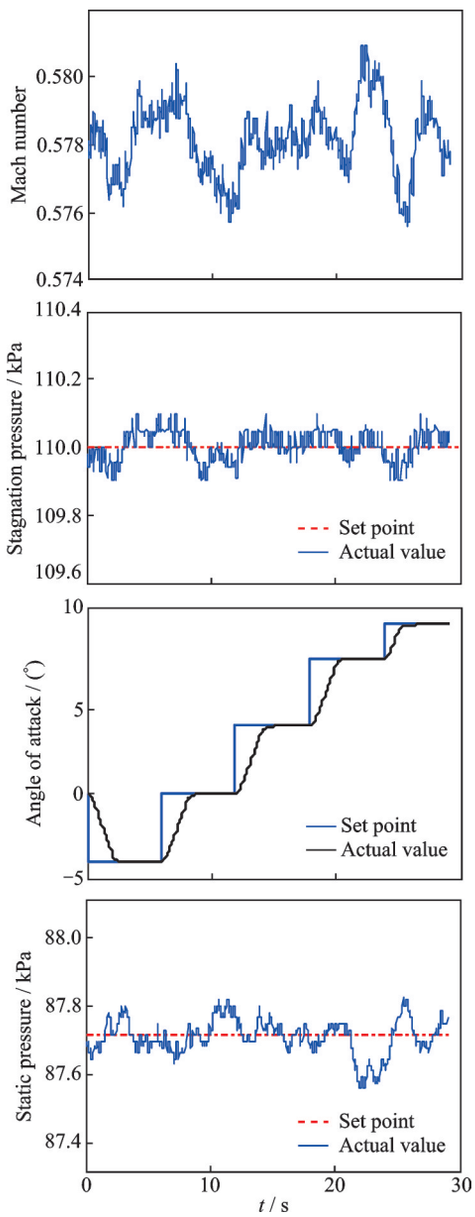

Fig.8 Control performance of simple DMC controller when Ma=0.578

4.2.3 Repeatability experiments

To verify the repeatability of the proposed method, three experiments are conducted under the condition when Ma=0.714 and the stagnation pressure is 130 kPa. Table 6 indicates the control criteria of the three experiments, and the actual control performances are shown in Figs.9—11. The similar results illustrate that the proposed method is effective in different working conditions

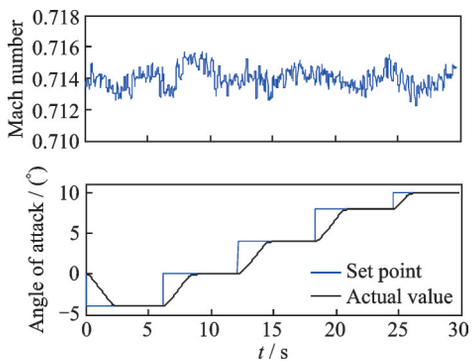

Fig.9 Process output of the first experiment of Ma= 0.714

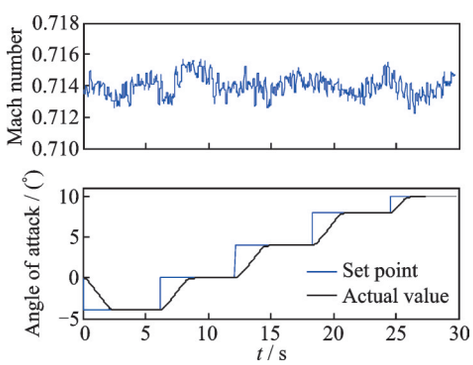

Fig.10 Process output of the second experiment of Ma=0.714

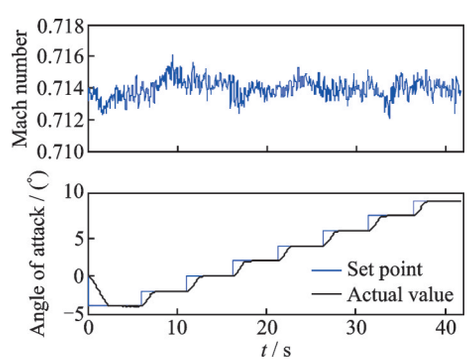

Fig.11 Process output of the third experiment of Ma=0.714

Table 6 Control criteria under the condition of Ma=0.714

Serial number	E		σ		MPE		MNE	
	δ_{Ma}	TP/kPa	δ_{Ma}	TP/kPa	δ_{Ma}	TP/kPa	δ_{Ma}	TP/kPa
1st	0.000 5	0.010 6	0.000 7	0.060 6	0.001 7	0.211 9	−0.002 0	−0.160 2
2nd	0.000 6	0.005 9	0.000 6	0.062 4	0.002 0	0.222 3	−0.001 8	−0.139 6
3rd	0.000 5	0.005 1	0.000 6	0.052 8	0.002 1	0.156 4	−0.001 9	−0.174 4

4.2.4 Experiments under different mach numbers

To further exam the proposed controller (DMC with feedforward), it is used in the tests of Ma=0.675 and Ma=0.822. Table 7 indicates the criteria of the proposed controller under two set points of Mach numbers (0.675 and 0.822). Taking into account Table 5 and Table 7, we can find the proposed controller can guarantee more than half of the sampling Mach numbers reach target precision (0.001). Fig.12 and Fig.13 show the process response at Ma=0.675 and Ma=0.822, respectively.

Note that, for saving experiment cost and reducing experiment times, the controller of Ma=0.675 is designed and tuned according to the step response data of Ma=0.714. Therefore the experimental results demonstrate the proposed method holds robustness as well.

Table 7 Control criteria of the proposed controller at Ma=0.675 and Ma=0.822

Set point	E		σ		MPE		MNE	
	δ_{Ma}	TP/kPa	δ_{Ma}	TP/kPa	δ_{Ma}	TP/kPa	δ_{Ma}	TP/kPa
Ma=0.675, p_0=130 kPa	0.000 5	0.010 6	0.000 7	0.060 6	0.001 7	0.211 9	−0.002 0	−0.160 2
Ma=0.822, p_0=130 kPa	−0.000 5	0.006 9	0.000 7	0.059 4	0.002 3	0.170 3	−0.002 4	−0.170 9

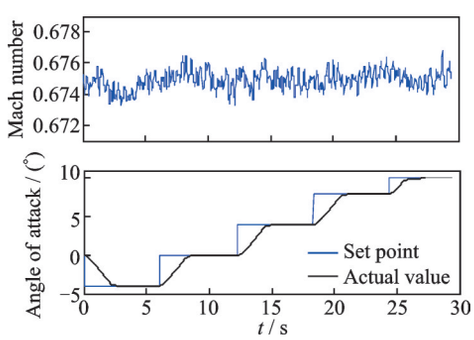

Fig.12 Process response when Ma=0.675

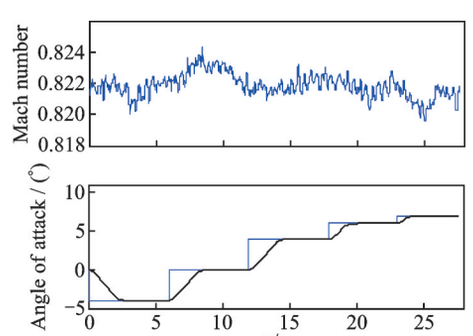

Fig.13 Process response when Ma=0.822

The feedforward-compensated DMC wind tunnel Mach number controller exhibits superior robustness and strong adjustment capability under similar operating conditions. It employs predictive control based on the system's dynamic model, effectively addressing parameter variations and external disturbances. Additionally, feedforward compensation enables the controller to respond to disturbances in advance, reducing sensitivity to such disturbances, while optimization algorithms allow for real-time adjustments to the control strategy. These factors collectively enhance the controller's performance across different conditions, ensuring it maintains good adjustment capability even under similar operating scenarios.

5 Conclusions

A new control system structure with smaller lag and less nonlinearity is designed for an intermittent transonic wind tunnel in CARDC. In order to improve the precision of the wind tunnel flow field, a feedforward and feedback multivariable DMC is designed for maintaining the Mach number and the stagnation constant during the attack angle varying. By tuning the parameters of the controller, the Mach number precision in wind tunnel tests is controlled within 0.001. It is verified that this control method is effective for high-precision flow field regulation through the real blowing tests under different conditions which are Ma=0.578, 0.714, 0.675 and 0.822. In the future, we can study the deep integration of intelligent methods

such as neural network and fuzzy logic with DMC method with feedforward to solve the shortcomings of traditional linear model in describing nonlinear and time-varying models, and combine intelligent optimization algorithm to realize parameter self-tuning and reduce the burden of manual parameter debugging.

References

[1] NOTT C R, ÖLÇMEN S M, LEWIS D R, et al. Supersonic, variable-throat, blow-down wind tunnel control using genetic algorithms, neural networks, and gain scheduled PID[J]. Applied Intelligence, 2008, 29(1): 79-89.

[2] ZHANG G J, CHAI T Y, SHAO C. A synthetic approach for control of intermittent wind tunnel[C]// Proceedings of the 1997 American Control Conference. Albuquerque, USA: IEEE, 2002: 203-207.

[3] SOETERBOEK R A M, PELS A F, VERBRUGGEN H B, et al. A predictive controller for the Mach number in a transonic wind tunnel[J]. IEEE Control Systems Magazine, 1991, 11(1): 63-72.

[4] LINDAHL P, MOOG E, SHAW S R. Simulation, design, and validation of an UAV SOFC propulsion system[J]. IEEE Transactions on Aerospace and Electronic Systems, 2012, 48(3): 2582-2593.

[5] SARUNIC P, EVANS R. Hierarchical model predictive control of UAVs performing multitarget-multisensor tracking[J]. IEEE Transactions on Aerospace and Electronic Systems, 2014, 50(3): 2253-2268.

[6] CUNNINGHAM J W, FISHER C H, PRICE L L. Density and temperature in wind tunnels using electron beams[J]. IEEE Transactions on Aerospace and Electronic Systems, 1967, AES-3(2): 269-284.

[7] KULKARNI S D, MINOR M A, DEAVER M W, et al. Design, sensing, and control of a scaled wind tunnel for atmospheric display[J]. IEEE/ASME Transactions on Mechatronics, 2012, 17(4): 635-645.

[8] DINCA L, CORCAU J I. A prototype for airflow speed control in a subsonic wind tunnel[J]. IEEE Aerospace and Electronic Systems Magazine, 2014, 29(2): 14-21.

[9] YANG S L, XU K J. Frequency-domain decoupling-correction method for wind tunnel strain-gauge balance[J]. IEEE Transactions on Instrumentation and Measurement, 2013, 62(9): 2596-2608.

[10] FU Y, CHAI T Y. Intelligent decoupling control of nonlinear multivariable systems and its application to a wind tunnel system[J]. IEEE Transactions on Control Systems Technology, 2009, 17(6): 1376-1384.

[11] RUI W, QIN J H, MA Y Y. A novel approach for modelling of an injector powered transonic wind tunnel[C]//Proceedings of the 26th Chinese Control and Decision Conference (2014 CCDC). Changsha, China: IEEE, 2014: 1197-1200.

[12] MIWA H, SATO M, SAKAKIBARA S, et al. Closed-loop Mach number control and measurement[C]//Proceedings of International Symposium on Fluid control and measurement, [S.l.]: [s.n.], 1985: 515-520.

[13] MOTTER M A, PRINCIPE J C. Predictive multiple model switching control with the self-organizing map[J]. International Journal of Robust and Nonlinear Control, 2002, 12(11): 1029-1051.

[14] ZHANG T F, MAO Z Z, YUAN P. Decoupled PID controller for wind tunnel system[C]//Proceedings of the 26th Chinese Control and Decision Conference (2014 CCDC). Changsha, China: IEEE, 2014: 3547-3550.

[15] HWANG D S, HSU P L. A robust controller design for supersonic intermittent blowdown-type windtunnels[J]. The Aeronautical Journal, 1998, 102 (1013): 161-170.

[16] PELS A F. Closed-loop Mach number control in a transonic wind tunnel[J]. Journal A, 1989, 30(4): 25-32.

[17] RICHALET J, RAULT A, TESTUD J L, et al. Model predictive heuristic control applications to industrial processes[J]. Automatica, 1978, 14(5): 413-428.

[18] CULTER C R, RAMAKER B C. Dynamic matrix control—A computer control algorithm[C]//Proceedings of Joint Automatic Control Conference, [S.l.]: [s.n.],1980.

[19] TAO J L, ZHU Y, FAN Q R. Model predictive control for a class of systems with isolated nonlinearity[J]. ISA Transactions, 2014, 53(4): 1343-1349.

[20] KUMAR D, BUDMAN H. Robust nonlinear MPC based on volterra series and polynomial chaos expan-

sions[J]. Journal of Process Control, 2014, 24(1): 304-317.

[21] QIN S J, BADGWELL T A. A survey of industrial model predictive control technology[J]. Control Engineering Practice, 2003, 11(7): 733-764.

[22] WANG L M, CHENG Y, ZOU J. Battery available power prediction of hybrid electric vehicle based on improved dynamic matrix control algorithms[J]. Journal of Power Sources, 2014, 261: 337-347.

[23] ÖZKAN G, ÜSER A, HAPOGLU H, et al. Experimental application of linear/nonlinear dynamic matrix control to a reactor of limestone slurry titrated with sulfuric acid[J]. Chemical Engineering Journal, 2008, 137(2): 320-327.

[24] MOON U C, LEE K Y. Step-response model development for dynamic matrix control of a drum-type boiler-turbine system[J]. IEEE Transactions on Energy Conversion, 2009, 24(2): 423-430.

[25] KEMBER G C, DUBAY R, MANSOUR S E. On simplified predictive control as a generalization of least-squares dynamic matrix control[J]. ISA Transactions, 2005, 44(3): 345-352.

[26] MO S Y, WANG L M, YAO Y, et al. Two-time dimensional dynamic matrix control for batch processes with convergence analysis against the 2D interval uncertainty[J]. Journal of Process Control, 2012, 22(5): 899-914.

[27] CUTLER C R. Dynamic matrix control: An optimal multivariable control algorithm with constraints[D]. Huston, USA: University of Huston, 1983.

[28] VEERACHARY M, SENJYU T, UEZATO K. Feedforward maximum power point tracking of PV systems using fuzzy controller[J]. IEEE Transactions on Aerospace and Electronic Systems, 2002, 38(3): 969-981.

[29] ZHANG R D, LU J Y, QU H Y, et al. State space model predictive fault-tolerant control for batch processes with partial actuator failure[J]. Journal of Process Control, 2014, 24(5): 613-620.

[30] MAURATH P R, MELLICHAMP D A, SEBORG D E. Predictive controller design for single-input/single-output (SISO) systems[J]. Industrial & Engineering Chemistry Research, 1988, 27(6): 956-963.

[31] SHRIDHAR R, COOPER D J. A novel tuning strategy for multivariable model predictive control[J]. ISA Transactions, 1997, 36(4): 273-280.

[32] SHRIDHAR R, COOPER D J. A tuning strategy for unconstrained multivariable model predictive control[J]. Industrial & Engineering Chemistry Research, 1998, 37(10): 4003-4016.

Authors

The first author Mr. **DU Ning** received the M.S. degree in control engineering from Southwest University of Science and Technology in 2014. In 2007, he was a senior engineer with the Institute of High Speed Aerodynamics, China Aerodynamics Research and Development Center, Mianyang, China. His research interest includes automatic control and simulation.

The corresponding author Dr. **ZHU Wenjie** received the B.S. degree in electronic engineering and technology from Zhengzhou University in 2011 and received the Ph.D. degree in instrument science and technology from Mechanical Engineering University in 2014. He is an engineer with the Institute of High Speed Aerodynamics, China Aerodynamics Research and Development Center, Mianyang, China. His research interest includes system identification, modeling and automatic control.

Author contributions Mr. **DU Ning** contributed to algorithm development, supported the analysis, and revised the manuscript. Dr. **ZHU Wenjie** conceived the study, conducted the analysis, interpreted the results, and originally drafted the manuscript. Mr. **YAO Dan** contributed to text organization, review and editing. Ms. **ZOU Xinlei** contributed to the research background and review. Mr. **QIN Jianhua** provided critical insights during discussion. All authors commented on the manuscript draft and approved the submission.

Competing interests The authors declare no competing interests.

(Production Editor: WANG Jie)

用于暂冲式跨声速风洞流场的前馈动态矩阵控制器设计

杜　宁，朱文杰，姚　丹，邹欣蕾，秦建华

（中国空气动力研究与发展中心高速空气动力研究所，绵阳 621000，中国）

摘要：暂冲式跨声速风洞迎角变化过程中，马赫数与总压的高精度稳定控制是风洞试验的核心技术要求，现有PID（Proportional integral derivative）控制策略难以实现0.001的马赫数控制误差目标，且应对迎角快速变化引发的流场扰动的能力不足。本文以中国空气动力研究与发展中心暂冲式跨声速风洞为研究对象，针对其多输入多输出（Multi-input multi-output，MIMO）、大滞后、非线性的流场控制特性，重构了风洞控制系统结构，将引射压力增设为受控变量以削弱主调压阀至试验段的控制滞后，同时选取静压替代马赫数作为受控变量以降低马赫数与静压间的非线性耦合影响；基于风洞一阶加纯滞后过程模型，设计了适用于风洞流场的多输入多输出动态矩阵控制器（Dynamic matrix controller，DMC），并结合迎角变化的可预测性，引入前馈补偿策略以抑制迎角变化引发的试验段压力扰动；依据风洞不同马赫数下的模型参数，制定了包含采样时间、预测域、控制域等在内的控制器参数整定策略。通过马赫数0.578、0.675、0.714、0.822的实际吹风试验，对比验证了所提前馈动态矩阵控制策略与传统PID控制、无前馈补偿动态矩阵控制的控制性能，结果表明该策略将马赫数控制误差稳定在0.001范围内，总压控制精度与抗扰动能力也显著提升，且在不同马赫数工况下均表现出良好的重复性与鲁棒性。本文所设计的控制策略有效解决了暂冲式跨声速风洞攻角快速变化下的流场高精度控制难题，为高超声速风洞等复杂流体试验装置的流场控制提供了技术参考。

关键词：暂冲式跨声速风洞；流场控制；动态矩阵控制器；前馈补偿；多输入多输出系统；参数整定

研究亮点：

1. 针对暂冲式跨声速风洞，提出了一种新颖的控制系统结构。该结构通过引入引射压力作为被控变量以减小控制时滞，并选用静压而非马赫数作为被控变量，以削弱参数间的非线性耦合。

2. 设计了一种集成攻角前馈补偿的多变量动态矩阵控制器用于风洞流场控制。该控制器充分利用了攻角变化的可预测性，有效抑制了由攻角快速变化引起的试验段压力扰动。

3. 基于风洞在不同马赫数下的一阶加纯延迟模型，制定了一套完整且实用的动态矩阵控制参数（采样时间、预测时域、控制时域等）整定策略，实现了控制器参数针对不同工况的优化设置。

4. 在实际吹风试验中，所提出的控制策略能将马赫数偏差稳定控制在0.001以内，并显著提升了风洞流场的总压控制精度和抗干扰能力，在不同马赫数条件下均展现出优异的重复性和鲁棒性。